International Journal of Modern Manufacturing Technologies
ISSN 2067–3604, Vol. XII, No. 1 / 2020

INVESTIGATIONS ON EFFECT OF LASER HARDENING PROCESS PARAMETERS ON MICROHARDNESS AND TRIBOLOGICAL CHARACTERISTICS OF CAST IRON USING TAGUCHI TECHNIQUE

Santoshkumar Vasantrao Wagh[1], Dhananjay Vishnuprasad Bhatt[2], Jyoti Menghani[3]

[1]Assistant Professor, Mechanical Engineering Department, COEP, Pune-411005, India
[2]Professor, Mechanical Engineering Department, SVNIT, Surat-395007
[3]Associate Professor, Mechanical Engineering Department, SVNIT, Surat-395007

Corresponding author: Santoshkumar V. Wagh, waghsv@gmail.com

Abstract: In the present investigation, laser hardening of cast iron is optimized by using Taguchi's approach. Cast iron is widely used in various engineering applications in the area of surface wear. The surface laser hardening process is used mostly because of its beauty to harden the selective area without affecting surface properties of the remaining area. The experimental results in this study find that laser beam power is a more significant factor than the laser scan speed and standoff distance for both wear rate and micohardness analysis. The experimental results obtain the highest microhardness value of 837.60 HV0.3 and minimum wear value of 2.66 x 10^{-9} g/cm at laser beam power of 330 W, laser scan speed of 1 mm/s and standoff distance of 300 mm. The comparisons of Taguchi and experimental results show very small percentage deviations with their correlation coefficients (r^2) 0.973 for wear rate and 0.922 for microhardness which is good in agreeable.

Key words: Taguchi's approach, Cast Iron, Wear rate, Microhardness, Laser scan speed and Standoff distance

1. INTRODUCTION

Surface properties and wear resistance can be improved by laser hardening process. There are wide variety of industrial applications of laser hardening process for the mechanical components such as steering gear assemblies, diesel engine cylinder liner, turbine blades and stub axles to achieve maximum microhardness and to increase the wear resistance (Taltavull et al., (2013), Adel et al., (2014), and Nemecek et al., (2013)). Lusquinos et al. (2007) investigated the effect processing parameters like scanning speed and density power of the laser beam on the laser hardening of AISI 1045 steel by using a high power diode laser. In this study, experiments have been carried out at 470, 650 and 760 W at scanning speed of 5, 10 and 15 mm/s respectively with focal length of 80 mm and spot of the laser beam over the surface of material which was 1.7 mm x 3.8 mm and achieved the hardness of 400-600 HV 100, the substrate hardness was 165-255 HV 100. The hardness of the laser treated surface increased two times more compared to the substrate hardness after the laser surface hardness process. Santhanakrishnan and Kovacevic (2012) studied effects of process parameters on the formation of mixture of phases i.e. martensite, banite, ferrite and pearlite which affected on the uniformity of the depth hardness of laser treated tool steel AISI S7 at multi-pass laser treatment. They carried out the experiment on 2 kW high power direct diode laser (HPDDL) with changing laser power of 1400, 1600 and 1800 W, scan speed of 15, 20 and 25 mm/s of overlap 3.0 mm and achieved the hardness of 671, 776 and 795 $HV_{0.2}$ and heat treated depth of 150, 170 and 200 µm respectively. Rana et al. (2007) investigated the effects of process parameters on hardness and microstructure of three different carbon steels groups, in which there were variations in the carbon percentage. A 5kW CW CO_2 laser system used for the experiments with laser power range 2.2, 2.1 and 1.97 kW, transverse speed of 6, 8 and 12 mm/s and spot size of outer and inner diameter of 6.3, 2.27 mm and microhardness achieved for 0.28 % C steel 151, 296 and 155 HV, for 0.40% C steel 501, 190 and 217 HV and 0.46 % C steel 370, 710 and 244 HV. It has been observed that transverse speed is the most influencing parameter on the hardness and if the carbon percentage increases, the hardness value increases too. Taltavull et al. (2013) investigated the results of laser surface melting treatment using a high-intensity diode laser on AM60B Mg alloy steel; its wear resistance was tested using a pin on a dry sliding disc. The wear behavior of laser treated and without laser treated specimen was observed at various wear conditions. They did not observe severe plastic deformation for the specimen which is trated by laser. Monteiro et al. (2009) investigated effects laser surface treatment process increased wear resistance producing a surface layer of altered

microstructure. The outcome of this research work was to optimize process parameters like wavelength, operation mode, power, laser beam diameter and material properties and to find out characteristics of laser superficial hardening of cast iron. The experiments were performed on pearlitic gray cast iron used in various automobile industries. The laser surface treatment process did not change the surface roughness but it improved wear resistance after laser hardening. Adel (2014) evaluated characteristics of steel alloy CK45 using dry sliding wear with a process of laser surface hardening. He concluded that value at the maximum energy of 0.64 J there is a considerable rising in hardness and after laser hardening process, found dry sliding wear resistance value highly increasing. The processing parameters, laser beam size, laser energy and melting surface control produced fine microstructure and achieved hardness up to 850 HV. Adel et al. (2009) investigated the laser hardening process effect on acicular bainitic ductile iron on the friction and wear characteristics. They focused on how changes occur in surface properties of acicular bainitic ductile iron after laser hardening process at all loads, sliding speed and sliding time that increased for the wear resistance for production and structural part repair. Nemecek (2013) carried out laser surface hardening on cast iron with formation of martensite and carbide based phases, which improved the hardness values above 800- 900 HV (i.e. 64-67 HRC) and found lower hardness values due to formation of retained austenite. Benyounis et al. (2005) evaluated the effect of laser surface melting of nodular cast iron by using a 100 W Nd:YAG laser beam machine leads to dissolve majority of the graphite nodules and resolidification of fine dendritic structure comprising retain austenite and some martensite and cementite Fe_3C. They achieved 0.5 mm melted depth and hardness range of 500 to 600 HV by using laser surface treatment process. Gadag et al. (1995) investigated effects of laser power and scan rate on laser hardening of structural ductile iron by CO_2 laser, they concluded that the hardness increased with increasing beam power and decreasing scan rate and a linear relationship between the hardness and energy intensity was found. The maximum hardness achieved was 700 HV compared to surface hardness of base material of 270 HV with laser process parameters like laser power of 2000 W and scan rate of 18 mm/s and beam diameter of 2.0 mm respectively. Borowski and Bartkowiak (2010) considered wear behaviours and hardness of 6082(PA4) and aluminum alloys AlSi6Cu4 laser treated at laser power 400 and 530W with varius the traverse velocity from 2.8 to 5.33 mm/s no causing a considerable raise of roughness and such a surface roughness does not require any more additional machining. The hardness of laser treated samples, alloy AlSi6Cu4 improved from a level of 60-80 $HV_{0.1}$ to a level of 120 $HV_{0.5}$ and further rise in the hardness at laser treated zone to a level of 160 HV and for in alloy 6082 showed the increase hardness was smaller, up to a level of 120 $HV_{0.5}$. Qiu and Kujanpaa (2011) witnessed special effects of laser power and its density on transformation of hardening medium-carbon steel with a fiber laser. Fiber laser is a potential tool to produce high surface hardness and high hardened depth for medium carbon steels. Babu et al. (2012) applied laser transformation process for low alloy steel i.e. EN25 Steel and which is useful for automobile, aircraft and transportation industries. The effects of laser process parameters on the microstriucture and hardness for laser hardening process of EN25 steel by 2kW CW Nd:YAG laser system were used for experimentations with varying laser power of 750-1250 W and work table travel speed of 500-1000 mm/min. The hardness achieved by laser hardening process 782 $HV_{0.5}$ which is two times the base material hardness of 360-380 $HV_{0.5}$. Roy and Manna (2000) carried out the mathematical modeling to envisage optimum settings of laser surface hardening of austempered ductile iron that shows complete dissolution of graphite nodules in a martensitic microstructure of the laser hardening zone. Shin and Yoo (2008) evaluated the major effects of surface treatment by laser on microhardness and microstructure of hot-work tool steels by using CW Nd: YAG laser system which was used as a heat source. The laser surface treatment process parameter used is of laser power of 1095 W, with travel speed of 0.3 m/min and focal position of 02.0 to +2.0 mm respectively and it achieved hardness value 800 $HV_{0.5}$, compared to the parent material hardness values which was observed around 210 $HV_{0.5}$. Barka and Abderrazak (2015) studied an effective procedure of statistical analysis i.e. a systematic design of final tests which was performed by using Taguchi's matrix that is L_9 orthogonal array and the experiments results for modeling to investigate the effect of laser hardening process parameters on the case depth of 4340 steel cylindrical specimen. Jerniti et al. (2016) studied predictive modeling which is developed based on artificial neural network and regression evaluation of laser hardnening for cylindrical metal workpieces. Jean and Tzeng (2003) investigated the control of laser hardnening process parameters during the case hardening of cast iron by using Taguchi's method and multiple regression analysis for process optimization in high energy electron beam. Wagh et al. (2018) investigated effects of laser surface hardening process parameters on wear and mechanical properties of laser hardened alloy

steel CK45 by applying Taguchi's orthogonal array method, and using 400 W optic fiber laser system. Maximum microhardness and least wear rate was at 270 mm standoff distance, 10 mm/s laser scanning speed and 260W laser power. Maximum microhardness values of laser treated Ck45 steel obtained 688.10 to 884.80 $HV_{0.3}$ compared to the base metal microharness 249.00 to 258.00 $HV_{0.3}$ was observed. Badkar et al. (2011) used Taguchi's method and utility concept to optimize process parameters as laser scan speed, power and focused position and concluded that among these parameters, laser power had maximum effect on the hardened width and hardened depth of laser transformation hardening of commercially pure titanium. Ming-der and Yih-fong (2004) applied Taguchi's method to optimize process parameter travel speed of 35 mm/s, accelerating voltage of 5 KV and electrical current of 6 mA and summarized that among these, travel speed has maximum effect on the wear resistance of electron beam surface hardening of cast iron. The hardness of the laser treated layer was maximized to 900 HV and the base material was 200 HV. Jeyaraj et al. (2015) reported the optimization of flame hardening process parameters for medium carbon steel by using Taguchi's approach, and L_9 orthogonal array. The flame hardening process parameters were temperature like temperature of 750, 850 and 950 degree Celsius, standoff distance of 10, 20 and 30 mm and quenching time of 10, 52 and 50 seconds respectively optimized by using Taguchi's approach to maximize the microhardness value up to 801 HV as the parent material microhardness observed was 242 HV. They concluded that the quenching time was the most significant process parameter. Menghani et al. (2017) used Taguchi's technique to optimize the process parameters of Cr2O3 plasma thermal spray coating and Ni based hard facing alloy coating. The coating was developed by depositing the material by hardfacing with the help of manual metal welding on SS304 material. The process parameters were impact angle, impact velocity and feed rate and they concluded that among these process parameters, feed rate had the most significant parameter which affected impact angle and erosion rate had the less involvement on wear rate. Wagh et al. (2019) studied the effect of laser hardnening process factors on surface properties of cast iron by using Taguchi's L9 orthogonal array. Experiments were conducted on cast iron material. From the investigations the most significant parameter was observed that, laser beam power compared to other selected parameters as well as laser scan speed affected the microhardness of laser hardened sample of cast iron. More et al. (2017) investigated significant factors responsible for slurry erosion wear using Taguschi's L9 orthogonal array, SS304 had the target material. They found that impact velocity was the most significant factor compared to other factors. Manoj et al. (2019) studied the corner error and the corner radius in the wire electro-discharge machining process using the slant type fixture on Hastelloy X for 00 and 300 angles machining of a triangular shape slot using Taguchi's L16 orthogonal array design method. Roy et al. (2017) Investigation of TiNiCu memory shape alloys machining features using wire electro-discharge machining and study of the effect of input process parameters on machine surface performance using Taguchi's L16 orthogonal array approach.

To maximize microhardness and minimize wear rate was the final aim of the laser hardening process. To obtain certain values of microhardness and wear rate accurately and repeatedly, parameters to be controlled have effect the process. In this process, to develop a correlation between process parameters and the output response like microhardness, microstructure and wear behavior was not known. In this regard the optimization techniques are most helpful for the identification of main controlling process parameters. Hence, in this research study, Taguchi's approach is implemented to check effects of laser beam power, laser scan speed and standoff distance on microhardrness, microstructure and wear rate.

2. STARTEGY OF EXPERIMENTATION

2.1 Materials and methodology

The % elemental composition of the material is presented in Table 1. Wheras, Figure 1 shows the SEM picture of the cast iron as base material which clearly indicates the microstructural arrangement.

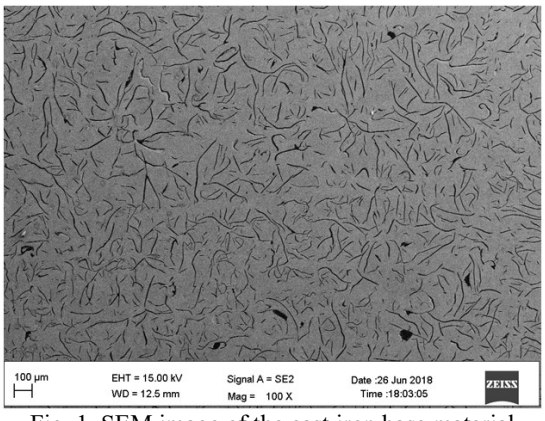

Fig. 1. SEM image of the cast iron base material

Table 1. Chemical composition (Wt. %) of material

Elements	C	Si	S	P	Mg
Composition weight %	3.65	1.71	0.067	0.176	0.38

2.2 Setup for conducting the experiments and preparation of specimen

Experimental trials were performed on 400 W optic fiber laser machine with a continuous wave (CW) mode SPI of 1070 nm laser wavelength, as demonstrated in Figure 2. Process parameters of laser hardening utilized laser beam power of 210, 270 and 330 W, laser scan speed of 1.0, 8.5 and 16 mm/s, also standoff distance of 200, 250 and 300 mm as indicated in Table 2. A 1.4 mm diameter of laser beam, argon gas was utilized at flow rate of 10 liter/minute.

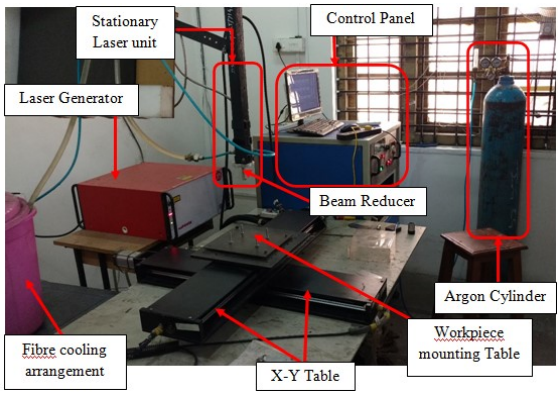

Fig. 2. Fiber laser machine 400 W of CW mode

For the sample preparation standard procedure was followed and the samples were cleaned by acetone. For the cutting of samples wirecut electrical discharge machine was utilised and samples are prepared into the size of 30 mm x 8 mm x 8 mm.

Table 2. Parameters and their level for laser hardening experiments

Sr. No.	Parameters	Unit	Level		
			1	2	3
1	Laser beam power (P)	W	210	270	330
2	Laser scan speed (S)	mm/s	1.0	8.5	16.0
3	Standoff distance (F)	mm	200	250	300

2.3 Microstructural analysis

In the present investigations, on the preset test specimens the laser tracks are marked according to the process parameters. After laser process, laser hardened samples were mirror polished with emery papers of different grades and 4% Nital was used for etching of the sample cross section. The hardened layer depth might have been observed for those with the aid of a microscope available in the lab. The microstructure of the hardened heat affected area had been investigated by utilizing microscope (SuXma Series, Conation Technologies, Pune). The microhardness of laser hardened specimens was measured by Vickers microhardness testing machine with test weight at a load of 300 g. The microhardness of the cast iron laser hardened specimens was checked by microhardness analyzer machine (Future Tech. Corp., Japan). The microhardness was measured on the surface and in addition over the laser hardened surface (i. e. along the area of the heat influenced zone).

2.4 Experimental Design

A distinctive design of experiment (DOE) practice was applied for analyzing vital influencing parameters and therefore the development of a model on the performance output was carried out. In laser surface treatment process, the output is micro-hardness which relies on three input parameters. Taguchi's style of experiments was thought-about, as a result, it is a lot of versatile than different analytical techniques in characteristic influenced every input parameter on microhardness.

For the present work three different parameters especially laser scan speed, power and standoff distance were used to check the microhardness as an output response of laser treated samples of cast iron. In the whole experiments, the testing parameter levels were utilized are indicated in Table 2. The working parameters, outcome signal to noise for every test run is demonstrated in Table 3. The test outcomes were transformed into to a signal to noise ratio.

The sign to noise ratio were computed for each variable level consolidation. The formula for the largest is a better S/N ratio using a base 10log as shown in equation (1).

$$\frac{\text{Signal}}{\text{Noise}} = -10 \log \frac{1}{n} \left[\sum \left(\frac{1}{y^2} \right) \right] \qquad (1)$$

where, n = number of observations; y = response for the given factors.

3. OUTCOMES AND DISCUSSION

3.1 Investigations on microhardness using Taguchi

To investigate the effect of process variables by Taguchi method, the present experimental results was analysed using MINITAB 14. Taguchi's L_9 orthogonal show S/N ratio for the investigation from microhardness test outcomes is demonstrated in Table 3. 'The larger the better' quality characteristic was chosen to get optimal conceivable parameters for the laser hardening technique.

The outcome response chart for those S/N ratios is depicted in Table 3. The laser beam power control was the foremost affecting critical control parameter among all the three parameters for causing the surface microhardness of cast iron as indicated in Table 4. The two parameters specifically scan speed of laser and standoff distances were positioned at the 2nd and 3rd positions individually over impelling

the microhardness for cast iron surface.

Table 3. Exploratory Taguchi'sL9 framework for microhardness of laser treated specimens of cast iron

Sr. No.	Laser beam power, (W)	Laser scan speed (mm/s)	Standoff distance (mm)	Micro Hardness $HV_{0.3}$	S/N Ratio
1	210	1	200	742.10	57.40
2	210	8.5	250	677.10	56.61
3	210	16	300	646.50	56.21
4	270	1	250	767.40	57.70
5	270	8.5	300	702.30	56.93
6	270	16	200	680.60	56.66
7	330	1	300	837.60	58.46
8	330	8.5	200	816.40	58.24
9	330	16	250	747.70	57.47

Table 4. S/N proportion reaction table utilizing the bigger the better characteristic

Level	Laser beam power (W)	Laser scan speed (mm/s)	Standoff distance (mm)
I	56.74	57.86	57.44
II	57.10	57.26	57.26
III	58.06	56.78	57.20
Delta	1.31	1.08	0.23
Rank	1	2	3

Figure 3 shows graphical outcomes of the most impact plot for the signal to noise ratio. The microhardness was claimed for the cast iron might have been found to be higher for 330 watt trailed at laser scan speed and standoff distance is 1 mm/s and 200 mm respectively.

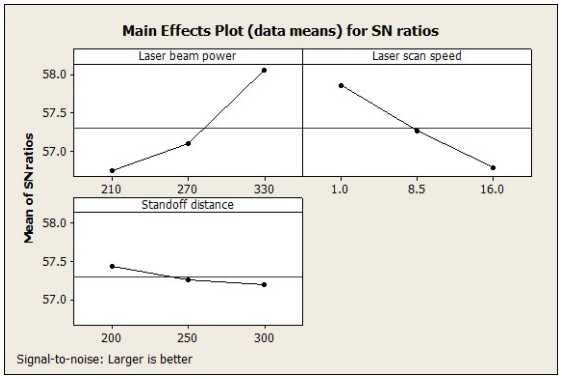

Fig. 3. Main impacts plot to signal to noise ratio

3.2 Impact of laser beam power control on microhardness

Table 3 indicates laser beam power control increments from 210, 270 and 330 W. At the consistent laser scan speed of 1 mm/s microhardness value increments for the laser treated cast iron sample. Table 3 reveals that microhardness value increments as 742.10, 767.40 and 837.60 $HV_{0.3}$ respectively and the most extreme microhardness achieved is 837.60 $HV_{0.3}$ which is two times higher than the base metal microhardness i.e. 258 $HV_{0.3}$.

3.3 Impact of laser scan speed control on microhardness

Table 3 indicates laser scan speed increments from 1.0, 8.5 and 16.00 mm/s at the consistent laser beam power of 330 W the microhardness values that diminishes for the cast iron laser treated sample. Table 3 reveals that microhardness esteem declines as 837.60, 816.40 also 747.70 $HV_{0.3}$, that intends those laser scan speed inversely proportional to microhardness. It may also be cleared from the chart pattern demonstrated in Figure 3.

3.4 Analyis of surface morphology

Microstructural analysis is adopted to analyse the surface morphology for the laser hardening surface which is processed with DOE. The microstructure of cast iron material observed the pearlite matrix, and the graphite flakes are shown in Figure 4(a), (b) and (c). The effective hardness width of 1018.67 µm and 1023. 78 µm was observed in the microstructure after the las er hardening process as shown in Figure 4 (b) and (c), respectively, acieved. Figure 4(b) microstructure shows acquired the least microhardness value of 646.50 $HV_{0.3}$ and maximum wear rate of 10.33 x $10^{9.0}$ g/cm at laser beam power control of 210 W, 16 mm/s laser scan speed and 300 mm of standoff distance among the test sets demonstrated in Table 3. Figure 4(c) highlights the microstructure of the laser treated samples for which it obtained maximum microhardness of 837.60 $HV_{0.3}$ and minimum wear rate values of 2.66 x $10^{-9.0}$ g/cm at laser beam power of 330 W, laser scan speed 1.0 mm/s and standoff distance 300 mm respectively.

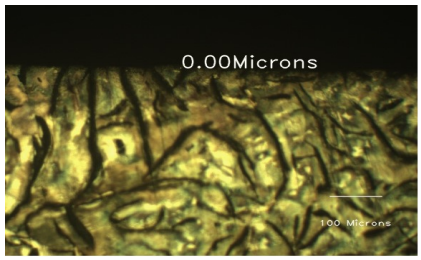

(a) Microstructure of base metal

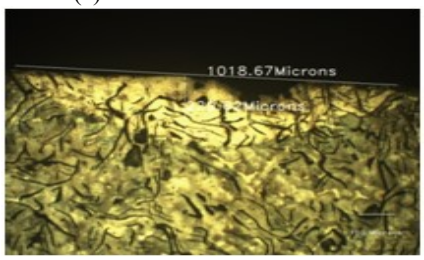

(b) Microstructure of laser hardened sample, at P = 210 W, S = 16 mm/s and f = 300 mm

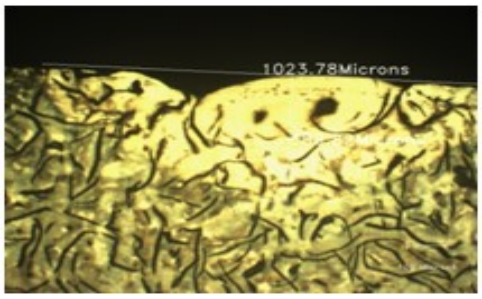

(c) Microstructure of laser hardened sample, at P = 330 W, S = 1.0 mm/s and f = 300 mm

Fig. 4. Microstructure of (a) Cast Iron base metal, (b) and (c) Cast Iron samples after laser hardening

3.5 Microhardness predication using predictive equation

The microhardness of the laser hardened specimens because of laser beam power might have been predicted utilizing the nonlinear equation for demonstrating the comparison between those micro-hardness consolidated effects of control parameters. This regression study was carried out by using Minitab 14 Software. The following form of the regression equation was obtained is shown in equation (2):

$$\text{Microhardness} = 579 + 0.933 \cdot P - 6.05 \cdot S - 0.176 \cdot F \quad (2)$$

where: P = Laser beam power, [W]; S = Laser scan speed, [mm/s]; F = Standoff distance, [mm].

The values of all the constants were calculated by utilizing Minitab 14 Software and by using these values in equation (2). The exactness of the calculated constants was affirmed from the value of correlation coefficient [r^2] of 0.922 which was got from the mathematical statement (2). The comparison between the microhardness got from the exploratory condition is as given in Table 5. A confirmation test was performed on cast iron sample by considering responsible parameters for obtained the maximum microhardness value. The microhardness obtained in the cast iron material due to the laser hardening process by using both nonlinear regression equation and confirmation experimental results are shown in Table 6. By comparing the experimental results and analytical results, deviation of about 3.11 % was found which is agreeable. Therefore, the developed regression equation is able to describe the microhardness of the laser treated cast iron material with various control factors with a reasonable degree off approximation.

Table 5. Microhardness by experimentation Vs prediction by equation

Expt. No.	Experimental result	Results from predictive equation	Percentage error (%)
1	742.10	733.68	1.14
2	677.10	679.51	0.35
3	646.50	625.33	3.38
4	767.40	780.86	1.72
5	702.30	726.69	3.35
6	680.60	698.91	2.61
7	837.60	828.04	1.15
8	816.40	800.27	2.01
9	747.70	746.09	0.21

Table 6. Confirmation of experimental results for microhardness of cast iron

Laser beam power (W)	Laser scan speed (mm/s)	Standoff distance (mm)	Micro hardness in test	Micro hardness by equation	% error
330	1	200	845.64	819.64	3.11

3.6 Wear analysis

In the present investigations Pin-on-disc sliding wear test is applied to investigate the performance of hardened surface against sliding wear. As per the laid down standard the wear test is conducted on cast iron untreated and laser treated samples. After and prior the wear test, the weight measurement of the samples was performed to study the weight loss during a dry sliding wear test. The Pin-on-disc apparatus for sliding wear testing is made by Ducom and the same test setup is shown in Fig. 5. The wear rate could be measured by a weight loss technique utilizing an analytical weight measurement machine. (Ana Matrix Instrument Technologic Pvt. Ltd., HZK-FA210) having a maximum capacity of 210 g, readability of $10^{-0.4}$g sensitivity. For wear rate calculation the relationship is given below in the said equation (3) [Adel et al. (2009) and Adel (2014)]:

$$\text{Wear rate} = \frac{\Delta W}{SD}\left(\frac{g}{cm}\right) \quad (3)$$

where,

ΔW = Weight loss, g

SD = Sliding distance, cm

$$\Delta W = W1 - W2$$

where,

W_1 = Initial weight of the test sample (g)

W_2 = Final weight of the test sample (g)

Initially the 10 N load was applied, with sliding speed of 450 rpm with sliding distance of 3000 m and the track diameter of 71 mm. The hardness of the counter disk was 63 HRC. The test is set up to run for 30 minutes this test was performed at normal room temperature.

Fig. 5. Pin on disc experimental set up of for wear testing

Table 2 shows the process variables and their levels applied for the experimentations. Those working parameters, effects and signal to noise ratio of every test run are demonstrated in Table 7. The experimental outcome values converted into a signal to noise ratio. The characteristics used in Taguchi's techniques are characterised by three categories for the signal to noise ratios. Those are the lesser the better, the nominal the best, the larger the better. In order to study the wear rate the smaller the better approach of S/N ratio is considered as shown in equation (4).

$$\frac{\text{Signal}}{\text{Noise}} = -10 \log \frac{1}{n}\left[\sum y^2\right] \qquad (4)$$

where: n = number of observations; y = response factor

L9 orthogonal array method shows signal to noise ratio for the examination of wear rate test outcomes demonstrated in Table 7. The S/N ratio responses calculated from equation (4) and are shown in Table 7. From the investigations it was observed that the among all three process parameters the laser power is the most responsible significant parameter for the minimum wear rate of cast iron. The Table 8 shows the ranking of significant responsible parameters 3rd for standoff distance, 2nd for laser scan speed and 1st is laser power.

Table 7. Design of experiments as per Taguchi's L9 matrix

Sr. No.	Laser beam power (W)	Laser scan speed (mm/s)	Standoff distance (mm)	Wear rate (g/cm) x 10^{-9}	S/N Ratio
1.	210	1	200	6.00	-15.56
2.	210	8.5	250	8.33	-18.41
3.	210	16	300	10.33	-20.28
4.	270	1	250	4.66	-13.36
5.	270	8.5	300	5.66	-15.05
6.	270	16	200	7.66	-17.68
7.	330	1	300	2.66	-8.49
8.	330	8.5	200	3.66	-11.26
9.	330	16	250	4.66	-13.36

Table 8. S/N ratio using the smaller the better criteria

Level	Laser beam power (W)	Laser scan speed (mm/s)	Standoff distance (mm)
I	-18.09	-12.48	-14.84
II	-15.37	-14.91	-15.05
III	-11.04	-17.11	-14.61
Delta	7.04	4.64	0.44
Rank	1	2	3

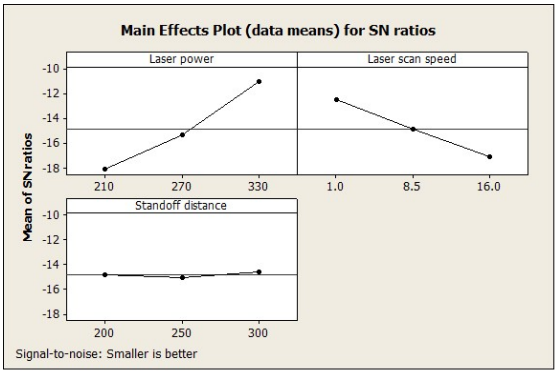

Fig. 6. Main effects of plot for S/N ratios

The Figure 6 represented the main effect plots of considerd process variables of the process on cast iron. The laser hardnening has remarkably improved the wear resistance of the cast iron and that is revealed in the investigations. The processing variables setting according to the L_9 orthogonal array is, 330 W of laser beam power, 1.0 mm/s scan speed and 300 mm of standoff distance. On the basis of the obtained results it can be noted that the wear rate of cast iron laser treated sample was influenced by process variables and their levels like laser power, laser scan speed and standoff distance.

3.7 Prediction of Wear rate using a analytical equation

The influence on the wear rate of the processing variables (laser power, stand-off distance and scan speed) of laser treated cast iron is anticipated by using a regression equation. This regression equation is used to show the relation between process variables and the wear rate calculated by pin on disk method. By regression analysis, the regression equation was obtained which is shown in equation (5).

$$\text{Wear rate} = 13.3 - 0.0380(P) + 0.207(S) + 0.00443(F) \quad (5)$$

where: P = Laser beam power, [W]; S = Laser scan speed, [mm/s]; F = Standoff distance, [mm]

The developed model is tested by means of the correlation coefficient and the obtained value of this coefficient is 0.973. This value shows good fitting of the model. This model is directly shows the error percentage between results obtained from predictive equation and rxperimental work as shown in Table 9.

Table 9. Wear analysis by experimentation Vs prediction by equation

Expt. No.	Results obtained from experiments, (g/cm) x 10^{-9}	Results obtained from predictive equation, (g/cm) x 10^{-9}	Percentage error (%)
1.	6.00	6.41	6.44
2.	8.33	8.19	1.75
3.	10.33	9.96	3.70
4.	4.66	4.35	7.02
5.	5.66	6.13	7.64
6.	7.66	7.24	5.83
7.	2.66	2.30	15.85
8.	3.66	3.41	7.47
9.	4.66	5.18	10.03

Table 10. Confirmation test for wear rate of cast iron

Laser beam power (W)	Laser scan speed (mm/s)	Standoff distance (mm)	Wear rate in test, (g/cm) x 10^{-9}	Wear rate by equation, (g/cm) x 10^{-9}	% error
330	1	300	2.40	2.30	4.53

After receiving the results of experimentations, a final confirmation test was executed on the same material, cast iron. The laser treated samples which are processed with optimum parametric settings where the wear rate was minimum is investigated again. This test shows minimum wear rate after the same wear test under designed conditions. The confirmation test was performed on cast iron laser treated and untreated samples. Table 10 shows the results of confirmation test, where it is cinfirming the result in negligible error, deviation of 4.53 % is found within an acceptable range. Therefore, from the above, it is observed that the regression equation is used to predict the wear rate value of the cast iron laser treated samples with respect to the proceesing variables and which shows control over the various process parameters with a sound degree of approximation.

3.8 Surface morphology of cast iron

The worn surface of the base material and laser hardened specimen examined at utilized load is 10 N, the sliding velocity of 450 rpm, sliding distance of 3000 m, rotating circular disc diameter of 71 mm. After the hardening process, the wear test is carried out on the pin on disk machine for all the samples treated as per DOE and one sample is also tested from parent untreated material. After wear test, the specimen from the wear scar section is removed from the respective sample and analyzed for the wear morphology with the help of SEM. Figure 7 (a) shows the wear morphology of the Cast Iron as received sample, the wear rate of plain Cast Iron observed is 7.38×10^{-7} g/cm. The wear morphology reveals that there are severe wear taking place on the untreated sample, which is mainly because of ploughing, delamination and micro cutting.

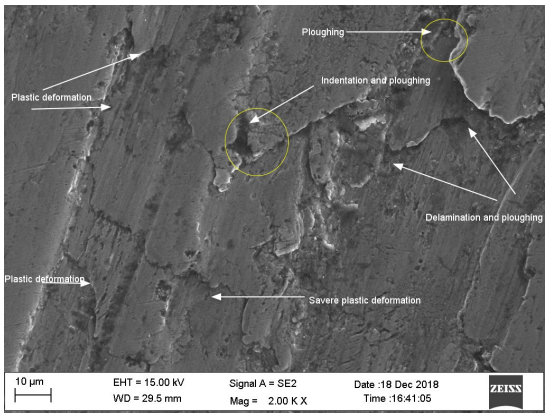

Fig. 7 (a). SEM image of the worn-out surface of Cast Iron as received (untreated)

Figure 7 (b) shows the SEM image of the worn out sample of experimental condition 3, where the wear rate is 10.33×10^{-9} g/cm. The processing condition is, P = 210 W, S = 16 mm/sec and F = 300 mm. The wear morphology shows micro-cutting, micro-indentation, plastic deformation, folded extruded tips and delamination. From all the considered experimental conditions this processing conditions shows a maximum wear rate which is attributed due to lower power and high scan speed and maximum standoff distance of laser.

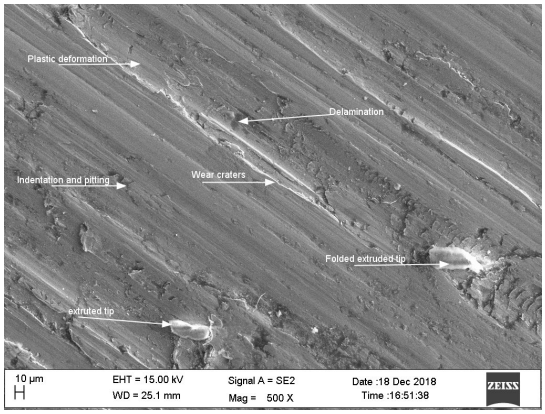

Fig. 7 (b) SEM image of the worn-out surface of Cast Iron treated as per the experimental condition at P = 210 W, S =1.0 mm/s and F = 300 mm.

Figure 7(c) shows the SEM image of the worn out sample of experimental condition 7, where the wear rate is 2.66×10^{-9} g/cm. The processing condition is, P = 330 W, S = 1.0 mm/sec and F = 300 mm. The wear morphology shows micro-cutting, micro-indentation, plastic deformation and delamination. From all the considered experimental conditions this processing conditions shows a minimum wear rate this is

attributed due to higher power and low scan speed and maximum standoff distance of laser.

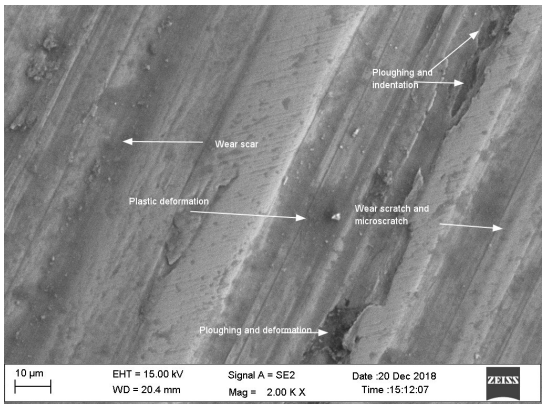

Fig. 7 (c). SEM image of the worn out surface of Cast Iron treated as per the experimental condition at P = 330 W, S = 1.0 mm/s and F = 300 mm.

4. CONCLUSIONS

In the present investigations, Taguchi's L9 orthogonal array is successfully applied to the optimization of laser process parameters to obtain maximum microhardness and minimum wear rate. Form the investigations, it is envisaged that the service life of cast iron components can be increased by applying laser surface hardness with optimum processing conditions. The surface properties like microhardness and microstructure improve and wear rate is minimised by controlling laser power, standoff distance and scan speed. The following conclusions are drawn from the results of the performed experimental studies.

The microhardness of the substrate (plain Cast Iron) is observed in the range of 258 $HV_{0.3}$ with wear a rate of 7.38×10^{-7} g/cm. The microhardness value of the obtained laser-treated cast iron steel sample is more than twice that of the untreated cast iron sample. From the experimental results obtained, the highest microhardness value is 837.60 $HV_{0.3}$, the minimum wear value of 2.66×10^{-9} g/cm with laser beam power 330 W, laser scan speed 1.0 mm/s, standoff distance is 300 mm.

From the S/N ratio analysis, it has been found that the microhardness value and wear value mainly depend on the process parameters with the rank order of the first rank of laser beam power, the second rank of laser scan speed and the third rank of standoff distance respectively. It is observed that, high laser power, low scanning speed and maximum standoff distance gives maximum microhardness during laser hardening and can produce maximum wear resistance.

The Cast Iron material treated with optimum conditions shows minimum wear rate of 2.40×10^{-9} g/cm, which is very less comparative to other processing conditions. The observed wear morphology shows micro-cutting, ploughing, micro-cracks, plastic deformation, folded lips, craters and delamination etc. The service life of cast iron componunts can be increases by applying laser surface hardness technique. The surface properties like microhardness and micro-structure improves and wear rate minimised by controlling laser power, standoff distance and scan speed.

5. ACKNOWLEDGMENTS

The present work was supported by Mechanical, Metallurgy and Material science department, COEP, Pune, Maharashtra, India- 411005. The authors are thankful to Mechanical Engineering Department, S V National Institute of Technology, Surat, India-395007 for their constant support.

6. REFERENCES

1. Lusquinos, F., Conde, J. C., Bonss, S., Riveiro, A., Quintero, F., Comesana, R., and Pou, J., (2007). *Theoretical and experimental analysis of high power diode laser (HPDL) hardening of AISI 1045 steel,* Applied Surface Science, **254**(4), 948-954.

2. Santhanakrishnan, S., and Kovacevic, R., (2012). *Hardness prediction in multi-pass direct diode laser heat treatment by on-line surface temperature monitoring*, Journal of Materials Processing Technology, **212**(11), 2261-2271.

3. Rana, J., Goswami, G. L., Jha, S. K., Mishra, P. K., and Prasad, B. V. S. S. S., (2007). *Experimental studies on the microstructure and hardness of laser-treated steel specimens,* Optics & Laser Technology, **39**(2), 385-393.

4. Taltavull, C., López, A. J., Torres, B., and Rams, J., (2013). *Dry sliding wear behaviour of laser surface melting treated AM60B magnesium alloy,* Surface and Coatings Technology, **236**, 368-379.

5. Monteiro, Waldemar A., Edmara MR Silva, and W. de Rossi., (2009). *Evaluation of the laser superficial hardening (LSH) in gray cast iron used in automobile industry,* In 3rd International Conference On Integrity, Reliability and Failure, Porto, Portugal, pp. 1-11.

6. Adel, K. M., (2014). *Enhancement of dry sliding wear characteristics of CK45 steel alloy by laser surface hardening processing*, Procedia materials science, **6**, 1639-1643.

7. Adel, K. M., Dhia, A. S., and Ghazali, M. J., (2009). *The effect of laser surface hardening on the wear and friction characteristics of acicular bainitic ductile iron,* International Journal of Mechanical and Materials Engineering, **4**(2), 167-171.

8. Nemecek, Stanislav., (2013. *Microstructure and properties of cast iron after laser surface hardening,* Materials Engineering-Materialove Inzinierstvo (MEMI), **20**(4), 153-159.
9. Benyounis, K. Y., Fakron, O. M. A., Abboud, J. H., Olabi, A. G., and Hashmi, M. J. S., (2005). *Surface melting of nodular cast iron by Nd-YAG laser and TIG,* Journal of Materials Processing Technology, **170**(1-2), 127-132.
10. Gadag, S. P., Srinivasan, M. N., and Mordike, B. L., (1995). *Effect of laser processing parameters on the structure of ductile iron,* Materials Science and Engineering: A, **196**(1-2), 145-154.
11. Borowski, J., and Bartkowiak, K., (2010). *Investigation of the influence of laser treatment parameters on the properties of the surface layer of aluminum alloys*, *Physics Procedia*, **5**, 449-456.
12. Qiu, F., and Kujanpaa, V., (2011). *Transformation hardening of medium-carbon steel with a fiber laser: the influence of laser power and laser power density*, Mechanics, **17**(3), 318-323.
13. Babu, P. D., Buvanashekaran, G., and Balasubramanian, K. R., (2012). *Experimental studies on the microstructure and hardness of laser transformation hardening of low alloy steel,* Transactions of the Canadian Society for Mechanical Engineering, **36**(3), 241-258.
14. Roy, A., and Manna, I., (2000). *Mathematical modeling of localized melting around graphite nodules during laser surface hardening of austempered ductile iron*, *Optics and lasers in engineering*, **34**(4-6), 369-383.
15. Shin, H. J., and Yoo, Y. T., (2008). *Microstructural and hardness investigation of hot-work tool steels by laser surface treatment*, Journal of materials processing technology, **201**(1-3), 342-347.
16. Barka, Noureddine, and Abderrazak El Ouafi., (2015). *Effects of laser hardening process parameters on case depth of 4340 steel cylindrical specimen- A statistical analysis,* Journal of Surface Engineered Materials and Advanced Technology **5**(3), 124.
17. Jerniti, Ahmed Ghazi, Abderazzak El Ouafi, and Noureddine Barka., (2016). *A predictive modeling based on regression and artificial neural network analysis of laser transformation hardening for cylindrical steel workpieces*, Journal of Surface Engineered Materials and Advanced Technology **6**(4), 149.
18. Jean, M. D., and Tzeng, Y. F., (2003). *Use of Taguchi methods and multiple regression analysis for optimal process development of high energy electron beam case hardening of cast iron,* Surface engineering, **19**(2), 150-156.
19. Wagh, S. V., Bhatt, D. V., Menghani, J. V., and Bhavikatti, S. S., (2018). *Effects of laser hardening process parameters on the mechanical and wear properties of ck45 steel using an orthogonal array*, International journal of modern manufacturing technologies, **10**(2), 86-93.
20. Badkar, D. S., Pandey, K. S., and Buvanashekaran, G., (2011). *Parameter optimization of laser transformation hardening by using Taguchi method and utility concept,* The International Journal of Advanced Manufacturing Technology, **52**(9-12), 1067-1077.
21. Ming-der, J., and Yih-fong, T., (2004). *Optimisation of electron-beam surface hardening of cast iron for high wear resistance using the Taguchi method*, The International Journal of Advanced Manufacturing Technology, **24**(3-4), 190-198.
22. Jeyaraj, S., Arulshri, K. P., Harshavardhan, K. P., and Sivasakthivel, P. S., (2015). *Optimization of Flame Hardening Process Parameters Using L9 Orthogonal Array of Taguchi Approach,* International Journal of Engineering and Applied Sciences, **2**(3).
23., J. V., Govande, A., and More, S. R., (2017). *Investigation on erosion wear behaviour of Cr_2O_3 plasma thermal spray coating and ni based hardfacing by welding with taguchi approach,* International journal of modern manufacturing technologies, **9**(2), 45-50.
24. Wagh, S. V., Ingole, S., Bhatt, D. V., Menghani, J. V., and Rathod, M. J., (2019). *Effect of Process Parameters on Surface Properties of Laser-Hardened Cast Iron,* In TMS 2019 148th Annual Meeting & Exhibition Supplemental Proceedings, Springer, Cham, 733-743.
25. More, S. R., Bhatt, D. V., and Menghani, J. V., (2017). *Study of the Parametric Performance of Solid Particle Erosion Wear under the Slurry Pot Test Rig*, Tribology in Industry, **39**(4), 471-481.
26. Manoj, I. V., Joy, R., Narendranath, S., & Nedelcu, D. (2019). *Investigation of machining parameters on corner accuracies for slant type taper triangle shaped profiles using WEDM on Hastelloy X*, IOP Conference Series: Materials Science and Engineering, 591(1), 012022.
27. Roy, A., Narendra, N., & Nedelcu, D. (2017). *Experimental investigation on variation of output responses of as cast TiNiCu shape memory alloys using wire EDM*, International Journal of Modern Manufacturing Technologies, 9(1), 90-101.

Received: February 09, 2020 / Accepted: June 15, 2020 / Paper available online: June 20, 2020